



TECHNISCHE  
UNIVERSITÄT  
WIEN  
Vienna University of Technology

## Marshal Plan Scholarship

Project report

### Design and characterization of novel amipolar host materials for organic electronic devices

**Dipl. Ing. Johannes Binting**

betreut von

**Univ.Prof. Dipl.-Ing. Dr.techn. Johannes Fröhlich**

Institut für Angewandte Synthesechemie,  
Technische Universität Wien, Getreidemarkt 9/163OC,  
A-1060 Wien

Juni 2013

Technische Universität Wien  
Vizekanzler für Forschung  
1040 Wien, Karlsplatz 13

1

---

Univ.Prof. Dipl.-Ing. Dr.techn.  
Johannes Fröhlich

## Table of Contents

<b>A)</b>	<b>Introduction &amp; Motivation .....</b>	<b>4</b>
<b>B)</b>	<b>Synthesis.....</b>	<b>8</b>
<b>C)</b>	<b>Device fabrication and characterization .....</b>	<b>11</b>
<b>D)</b>	<b>Indol[3,2,1-jk]carbazole (IC) investigations.....</b>	<b>17</b>
<b>E)</b>	<b>Conclusion .....</b>	<b>22</b>
<b>F)</b>	<b>Bibliography.....</b>	<b>23</b>

## Acknowledgements

First I would like to thank Prof. Pavel Anzenbacher Jr. and his research group for the possibility to conduct the here presented work in his laboratory.

Special thanks to Dr. Cesar Perez-Bolivar for his guidance, help and time offered to me through them. Without his extensive training and mentorship I would not have been able to acquire a new skill set in the field of organic electronic device fabrication and characterization. The success of this work is due in large part to his experience and foresight.

I also would like to thank my advisor, Prof. Johannes Fröhlich, for his support and guidance throughout this project.

I would like to extend my greatest appreciation to the Marshal Plan Foundation for the financial support and enabling me to realize this project and to grow as a member of the scientific community and as a person.

Finally, I would like to thank my spouse, Marlene Filipot, for all the love, strength and comfort she gave me during my time abroad.

## A) Introduction & Motivation

Due to inefficient illumination devices approximately 25% of electrical energy in Europe is used for lighting applications<sup>1</sup>. Old fashioned light bulbs convert only 5 % of the electric power into visible light and more efficient fluorescent tubes contain toxic mercury. While inorganic LEDs exhibit higher efficiencies, they are limited to point light sources and still depend on expensive rare earth elements.

In the context of climate change and the urgent need to reduce energy consumption, industry as well as academia is searching for ways to tackle this problem.

Organic light emitting diodes (OLEDs) are believed to be the answer for many of the above mentioned problems. OLED technology not only allows for more efficient lightning applications, but also allows fabrication of ultrathin flexible displays and solid state lighting panels thus creating entirely new ways of design and lifestyle.

Organic light-emitting devices are electroluminescence devices based on organic molecules. In the simplest case the organic emitting layer is placed between an electron inducing cathode and a hole inducing transparent anode. By applying a driving voltage, electrons are injected from the cathode into the lowest unoccupied molecular orbital (LUMO) of the adjacent organic layer, while the anode injects holes into the highest occupied molecular orbital (HOMO) of the organic material. If two of these opposite charges meet, they recombine to form an excited state called exciton (electron-hole pairs), which relaxes from the excited to the ground state and thus resulting in the emission of light (Figure 1). This process is called electroluminescence and is the basic principle of organic as well as inorganic light emitting devices<sup>2</sup>.

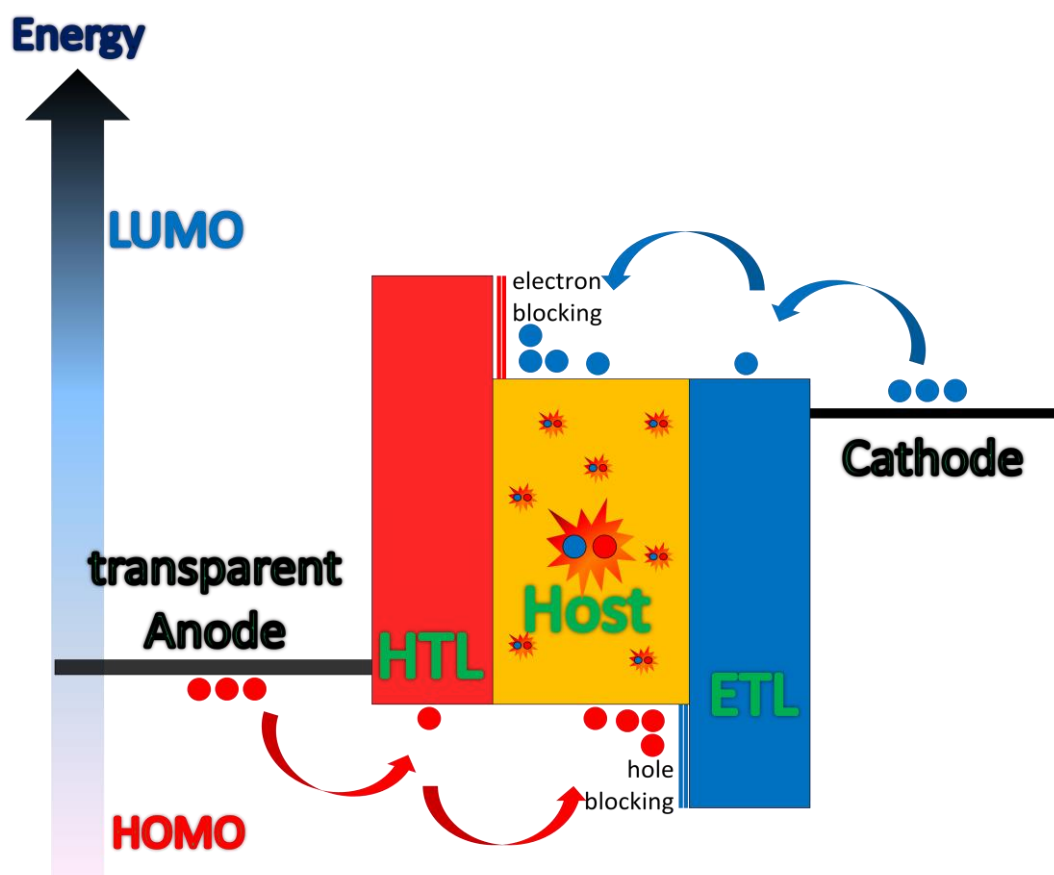


**Figure 1:** Scheme of an idealized multilayer PHOLED device: The staggered height of the layers indicates their different energies. Holes (red) are injected from the transparent anode into the HOMO level of the hole transporting layer (HTL), whose energy level has to be aligned with the HOMO of the host, whereas the HTL LUMO level has to be sufficiently high to prevent electron leakage from the host into the HTL. On the other side the electrons (blue) are injected from the cathode into the LUMO level of the electron transport layer (ETL), whose energy level has to be aligned with the LUMO of the host, whereas the ETL HOMO has to be sufficiently high to prevent hole leakage from the host into the ETL. Upon recombination in the host matrix, electron and holes form an excited state called exciton and transfer the energy to the phosphorescent dopants which emit light. Adapted scheme from Meerholz<sup>3</sup>

In an OLED device singlet- and triplet excitons are formed in a ratio of 1:3 under electrical excitation<sup>4</sup>. While first generation fluorescent OLEDs were intrinsically limited to efficiencies of only 25 %, phosphorescent organic light emitting devices (PHOLEDs) can harvest both singlet- and triplet- excitons simultaneously and therefore have the potential of 100 % internal quantum efficiency<sup>5</sup>.

PHOLED devices are realized by doping a heavy transition metal complex into a host matrix. Due to the strong spin-orbit coupling induced by the heavy metal elements, rapid intersystem crossing is promoted and consequently results in efficient emissive

decay from the lowest excited triplet state to the singlet ground state<sup>6</sup>. Ir(III) complexes are commonly used because of their high luminescent efficiency and intense phosphorescent emission combined with relatively short lifetime of the excited states<sup>7</sup>. In Figure 2 frequently used phosphorescent dopants along with their triplet energies are shown. Color tuning can be achieved by varying the complexing ligands.

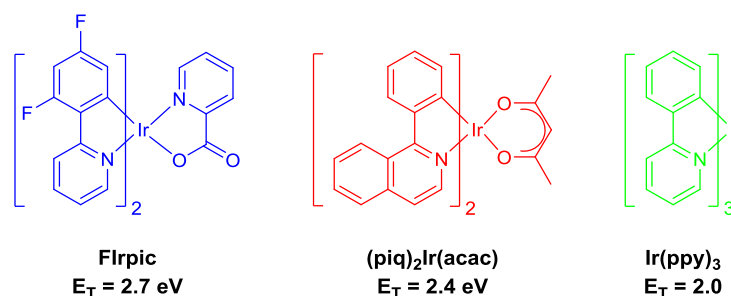


**Figure 2:** Red, blue and green Ir(III) complexes utilized as phosphorescent emitters in PHOLEDs<sup>8,9,10</sup>.

However, the phosphorescent dopants have to be dispersed and diluted in an organic host matrix in order to prevent triplet-triplet annihilation or non-radiative quenching processes as result of high concentrations<sup>11,12,13</sup>.

While red and green PHOLEDs have been successfully applied in commercial devices (Samsung Galaxy S3 & S4) the efficiency and lifetime of devices based on blue phosphorescent emitters is significantly lower. This is accredited to the stability and performance of the host material rather than the blue dopants.

Since blue light is inevitable for realizing high performance true color displays as well as white solid state lighting applications the development of stable and high performing novel blue host materials is considered to be the holy grail of PHOLED research.

Designing new host materials three key guidelines should be addressed: i) The host material should exhibit a higher triplet energy (E<sub>T</sub>) than that of the dopant in order to prevent reverse energy transfer from the guest back to the host, as well as to confine triplet excitons in the emissive layer. ii) The highest occupied molecular orbitals (HOMOs) and the lowest unoccupied molecular orbitals (LUMOs) energy levels of the host material have to be appropriately aligned with those of the neighboring active layers to facilitate injection of electrons and holes and guarantee a balanced charge transport. iii) The host material should have good thermal and morphological stability,

which is key to ensure stable working PHOLEDs and prolonged lifetime of the devices<sup>4,7,14,15</sup>.

Summing up, in order to develop highly efficient blue PHOLEDs host materials with a high triplet energy ( $E_T > 3.0$  eV) are required<sup>13,16</sup>. As a rule of thumb the triplet energy of the host should be 0.2-0.3 eV higher than that of the phosphorescent dopant in order to eliminate reverse energy transfer. However, materials possessing a combination of good charge-transport properties and high triplet energy are not always readily available. For example, the triplet energies of established hosts for green and red PHOLEDs such as Alq<sub>3</sub> ( $E_T = 2.30$  eV), BAlq ( $E_T = 2.45$  eV), TPBI ( $E_T = 2.65$  eV), CBP ( $E_T = 2.56$  eV), and TCTA ( $E_T = 2.76$  eV) are not suitable for deep-blue (~ 420 nm) phosphorescence applying Flrpic (2.65 eV)<sup>17,18</sup>.

To address this issue the Anzenbacher group investigated the widely used host material, 4,4'-Bis-(9-carbazolyl)-biphenyl (**CBP**) and showed that functional groups isomerism in **CBP** can lead to enhanced triplet energy while maintaining excellent charge transport properties.

As illustrated in Figure 3, substitution of the biphenyl moiety in positions 2 and 3 with carbazole increases the triplet-energy of the respective **CBP**-isomer.

The highest triplet energies are observed for 2,2' (**o-CBP**) and 2,3'-isomers, in which steric hindrance for planarization is highest and therefore preventing conjugation and triplet delocalization<sup>19,20</sup>.

While the **CBP** (4,4'-isomer) is not a suitable host for blue electro phosphorescence emitters, 3,3'-, 2,2'-, 2,3'- and 2,4'-isomers are potential candidates.

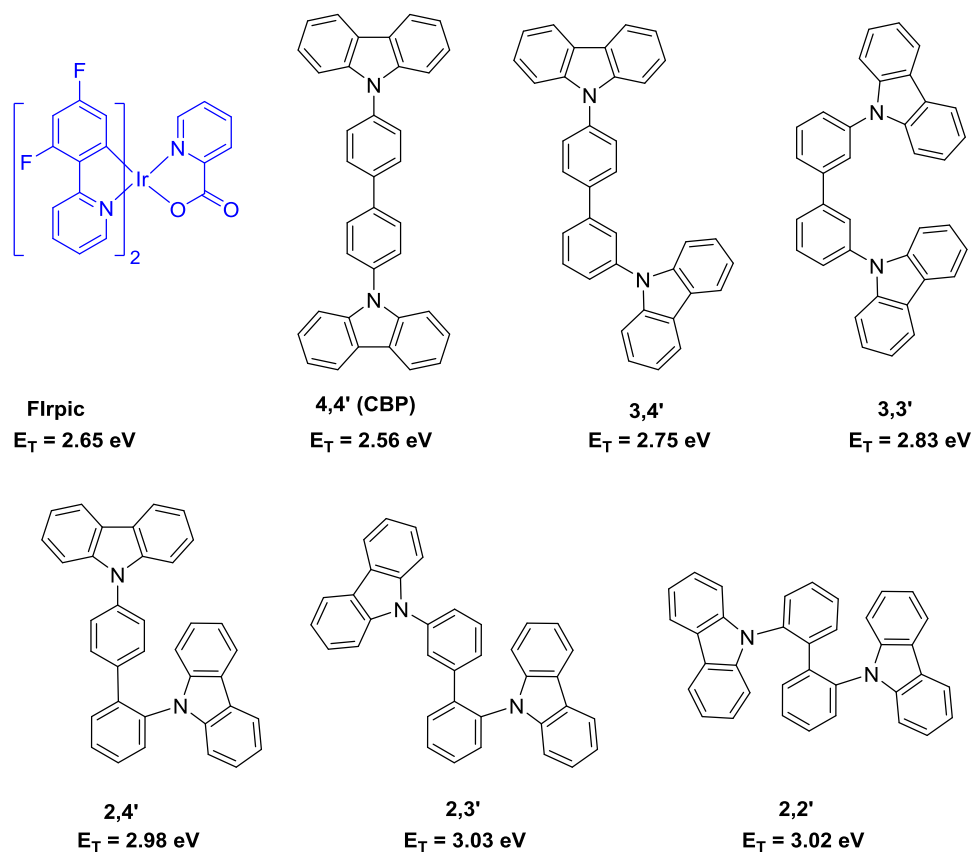
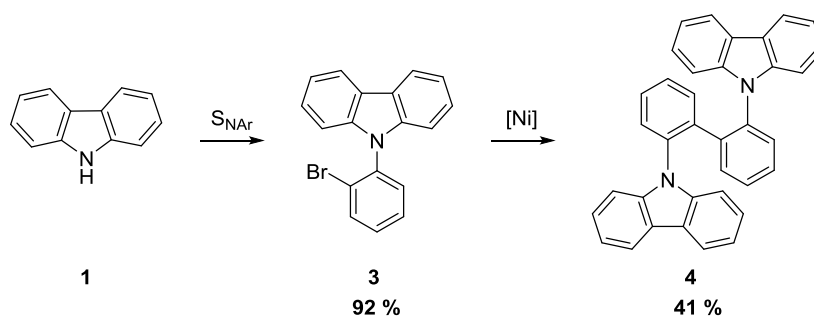


**Figure 3:** CBP isomers and their triplet energies; results of the combined concepts of planarization and o-linkage

## B) Synthesis

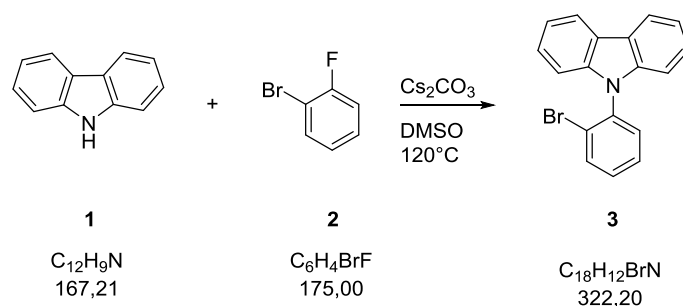
Target compound 2,2'-Di(9H-carbazol-9-yl)biphenyl (o-CBP) **4** was realized *via* a newly developed two step reaction protocol (Scheme 1), using the synthetic expertise of the Anzenbacher and Fröhlich group to give **4** in an overall yield of 38 %.



**Scheme 1:** newly developed two step protocol towards o-CBP



### 9-(2-Bromophenyl)-9H-carbazole **3**



Synthesis of **3** followed a protocol developed by the scholar during his diploma thesis<sup>21</sup>.

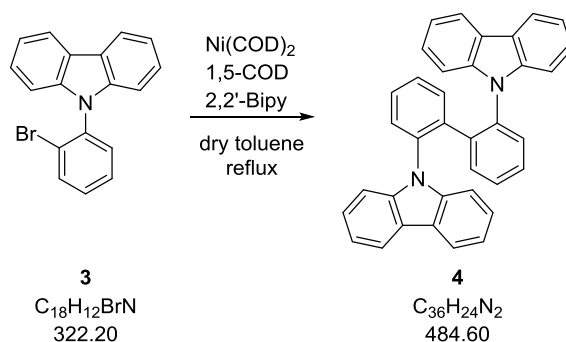
Carbazole **1** (1.17 g, 7 mmol, 1.0 eq) and 2-Bromofluorobenzene **2** (1.23 g, 7 mmol, 1.0 eq) were dissolved in DMSO (10 mL) before  $\text{Cs}_2\text{CO}_3$  (2.55 g, 7.84 mmol, 1.1 eq) was added to the solution under stirring. The suspension was stirred for 24 h at 120 °C. The solvent was removed under high vacuum before the reaction was extracted with DCM/H<sub>2</sub>O and dried with  $\text{Na}_2\text{SO}_4$ . The combined organic phases were removed by distillation under reduced pressure. Crystallization from EtOH yielded **3** as white solid (2.09 g, 92 %).

R<sub>f</sub> (PE:DCM=30:1)= 0.25

<sup>1</sup>H NMR (500 MHz, CDCl<sub>3</sub>, FID JBI239/10) δ ppm = 8.17 (2 H, d, *J*=7.57 Hz), 7.88 (1 H, dd, *J*=8.20, 1.58 Hz), 7.52 - 7.59 (1 H, m), 7.47 - 7.52 (1 H, m), 7.38 - 7.46 (3 H, m), 7.28 - 7.35 (2 H, m), 7.09 (2 H, d, *J*=7.88 Hz)

<sup>13</sup>C NMR (126 MHz, CDCl<sub>3</sub>, JBI239/40) δ ppm = 140.79 (s), 136.69 (s), 134.19 (d), 131.10 (d), 130.13 (d), 128.78 (d), 125.92 (d), 123.80 (s), 123.19 (s), 120.32 (d), 119.95 (d), 109.99 (d)

### 2,2'-Di(9H-carbazol-9-yl)biphenyl (o-CBP) **4**



In a flame dried, argon purged two neck round bottom flask 9-(2-Bromophenyl)-9H-carbazole **3** (0.967 g, 3 mmol, 1 eq) and Bis(cyclooctadiene)nickel(0) (0.325 g, 3 mmol, 1 eq) were suspended in dry toluene (20 ml). The resulting brown suspension was stirred and evacuated several times for 15 min till no more bubbles were observed. 2,2'-Bipyridine (0.469 g, 3 mmol, 1 eq) and 1,5-Cyclooctadiene (0.325 g, 3 mmol, 1 eq) dissolved in dry toluene (10 ml), were added dropwise under argon atmosphere. The reaction was evacuated and flushed with argon four times before it was heated until reflux under argon atmosphere over night. TLC control (Hex:EE=9:1) the following day indicated incomplete conversion. Additionally Bis(cyclooctadiene)nickel(0) (0.107 g, 0.39 mmol, 0.13 eq) was added in 1,5-Cyclooctadiene (7 ml). The reaction mixture was again evacuated and flushed with argon three times heated until reflux under argon atmosphere over night. The following day the reaction was filtrated and yielded pale yellow filtrate and black solid. The solvent was removed under vacuo and EtOH was added slowly till white precipitate was formed. The resulting solid was washed with EtOH and dried under high vacuum at 120°C at 0.5 mbar yielding beige solid 2,2'-Di(9H-carbazol-9-yl)biphenyl (o-CBP) **4** (0.300 g, 41 %).

$^1\text{H}$  NMR (500 MHz,  $\text{CDCl}_3$ , FID JBI236/20)  $\delta$  ppm = 7.87 (4 H, dd,  $J=7.88, 1.89$  Hz), (7.74 (6 H, br. s.)), 7.50 (4 H, td,  $J=7.65, 1.42$  Hz), 7.29 (4 H, td,  $J=7.72, 1.58$  Hz), 7.04 (4 H, dd,  $J=7.88, 1.26$  Hz), 6.99 (13 H, m); broad signals at 7.74 ppm and 6.99 ppm may come from Ni, although elemental analysis did not show Ni in the sample  
 $^{13}\text{C}$  NMR (126 MHz,  $\text{CDCl}_3$ , FID JBI236/30)  $\delta$  ppm = 140.39 (s), 137.88 (s), 136.03 (s), 133.41 (d), 128.95 (d), 128.85 (d), 128.04 (d), 124.97 (d), 123.69 (s), 119.43 (s), 119.32 (s), 110.05 (s)

MS calcd for  $\text{C}_{36}\text{H}_{24}\text{N}_2$  484.6, found 484.4

Elemental analysis: C 89.00 %, H 4.90 %, N 5.63 %

Compound **4** was sublimed two times at 160°C under high vacuum before being used as host material in a PHOLED device.

## C) Device fabrication and characterization

In order to test the o-CBP as host material for blue PHOLEDs several test devices applying blue phosphorescent emitter Flrpic were used. Furthermore, device architecture optimization for o-CBP:Flrpic host/guest-systems via electron transporting layer modifications were performed (Figure 4 and Figure 5). This approach for optimization is often used as charge transport in OLEDs is hole dominated. One side, preferably the hole transporting side is not modified while the electron transporting side is changed in order to screen for best performances.

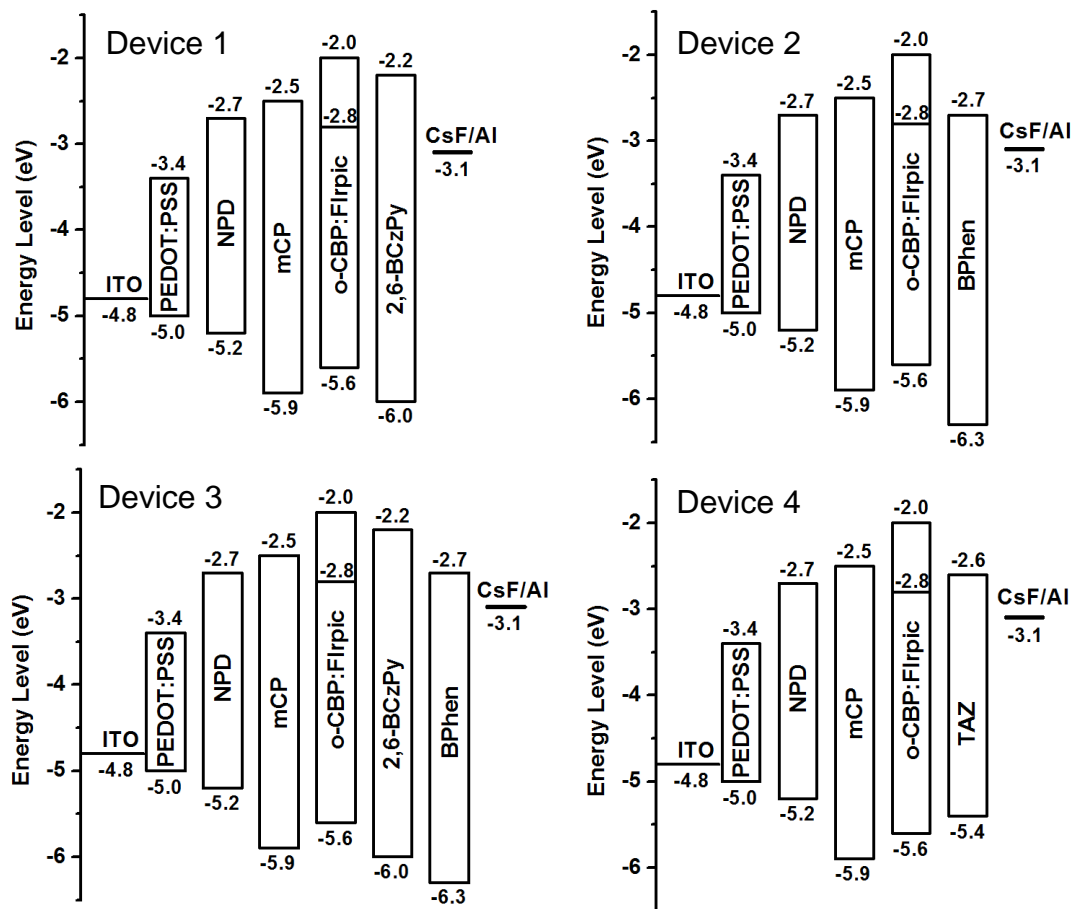


**Figure 4:** Energy level diagram of HOMO and LUMO levels (relative to the vacuum level) for the materials investigated in this work. Device 1: ITO/PEDOT:PSS/NPD(30nm)/mCP(5nm)/o-CBP(29nm):Flrpic(1.62)(5.3%)/26BCbzPy(35nm)/CsF(1.5nm)/Al(46nm)  
 Device 2: ITO/PEDOT:PSS/NPD(30nm)/mCP(5nm)/o-CBP(29nm):Flrpic(1.62)(5.3%)/Bphen(35nm)/CsF(1.5nm)/Al(46nm)  
 Device 3: ITO/PEDOT:PSS/NPD(30nm)/mCP(5nm)/o-CBP(29nm):Flrpic(1.62)(5.3%)/26BCbzPy(20nm)/Bphen(15nm)/CsF(1.5nm)/Al(46nm)  
 Device 4: ITO/PEDOT:PSS/NPD(30nm)/mCP(5nm)/o-CBP(29nm):Flrpic(1.62)(5.3%)/TAZ(35nm)//CsF(1.5nm)/Al(46nm)

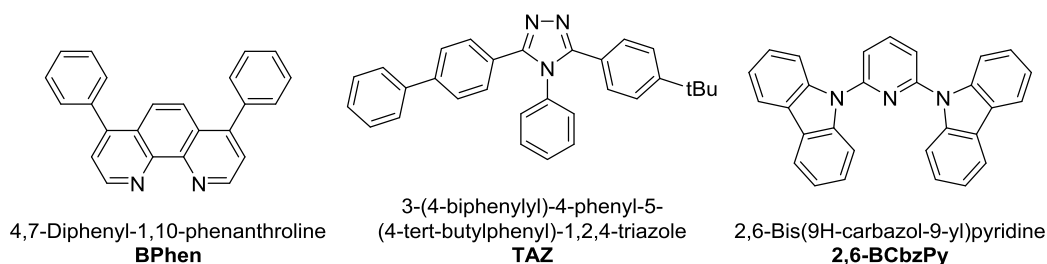


**Figure 5:** molecular structure of electron transporting materials BPhen, TAZ and 2,6-BCzPy

## Fabrication

In Table 1 the applied materials and corresponding thicknesses as well as fabrication parameters are listed.

Layer	Material	thickness [Å]	Rate [Å/s]	Power [%]	remarks	Device
1	ITO	3000	-	-	-	All
2	PEDOT:PSS	300	-	-	2000rpm/45s	All
3	NPD	300	0.50	8	193°C	All
4	mCP	50	0.25	7	85°C	All
5	o-CBP	290	0.45	8	87°C	All
5	Flrpic	162	0.03	Na	145°C	All
6	2,6-BCzPy	350	0.40	6	165°C	1
7	BPhen	350	0.40	6.3	115°C	2
8	2,6-BCzPy	200	0.40	6	166°C	3
8	BPhen	150	0.23	6	89°C	3
9	TAZ	350	0.28	1	129°C	4
10	CsF	150	0.1	14	-	All
11	Al	460	3.2	55	-	All

**Table 1:** Table of individual layer materials and their corresponding thicknesses, deposition rates and required power

All chemicals were purified at least two times through vacuum sublimation prior to use. The PHOLEDs were fabricated through vacuum deposition of the materials at  $10^{-7}$  Torr using a EvoVac Angstrom Engineering deposition system (Figure 6), existing of 8 individually controllable Radak sources allowing complex architectures of co-deposited materials onto ITO-coated glass substrates (sheet resistance of  $15 \Omega \text{ sq}^{-1}$ ). The ITO surface was degreased by detergent and cleaned ultrasonically; i.e. with acetone, isopropanol and deionized water in sequence, and finally with UV-ozone. Spin-coated poly 3,4-ethylenedioxythiophene:polystyrene sulfonate PEDOT:PSS (2000 rpm, 45s, 30 nm) was used as a hole injection layer, which was annealed at 140°C for 10min before the remaining layers were evaporated on top.

The deposition rate of each organic material was ca.  $0.2\text{-}0.5 \text{ \AA s}^{-1}$ . Subsequently, CsF was deposited at  $0.1 \text{ \AA s}^{-1}$  and then capped with Al (ca.  $3 \text{ \AA s}^{-1}$ ) through shadow masking without breaking the vacuum.

All the electrical and optical characterization of the diodes was performed with an integration sphere using C9920-12 External Quantum Efficiency Measurement System (Hamamatsu Photonics) and a Keithley 2400 sourcemeter. All the characterization of the devices was performed inside a nitrogen-filled glovebox.

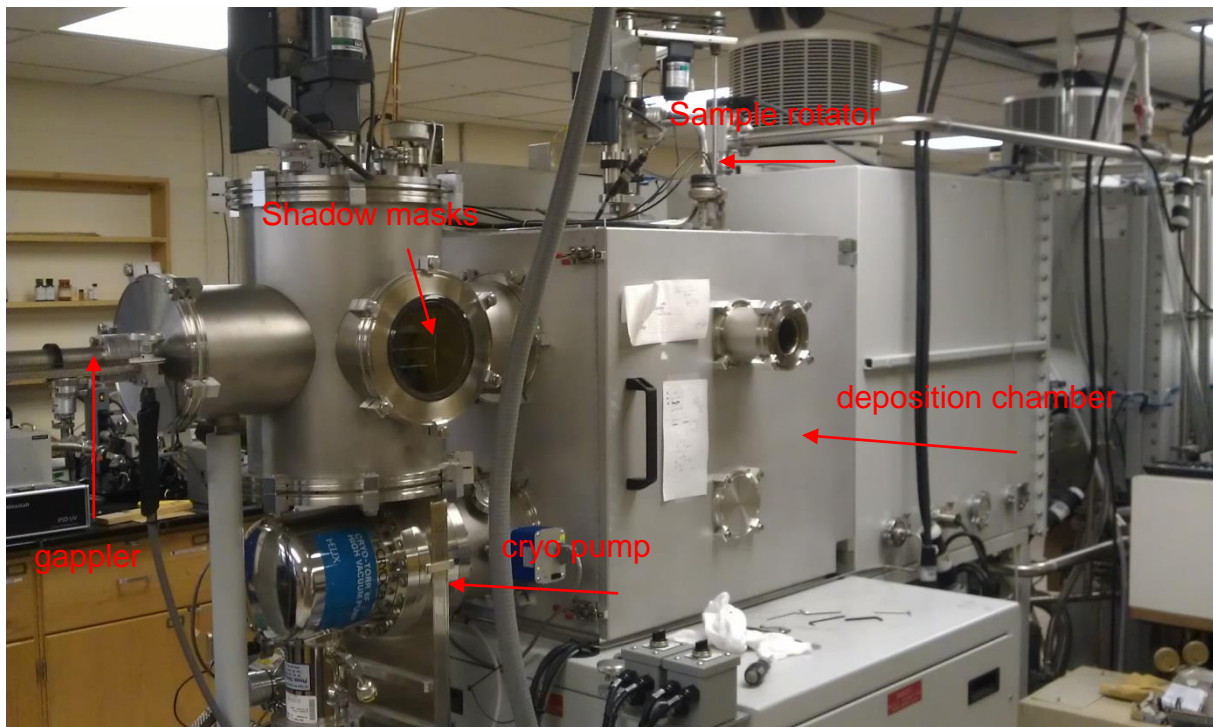


**Figure 6:** EvoVac Angstrom Engineering deposition system

## Results

A comparison of obtained current density-voltage-luminance (J-V-L) characteristics of devices 1-4 is illustrated in Figure 7.

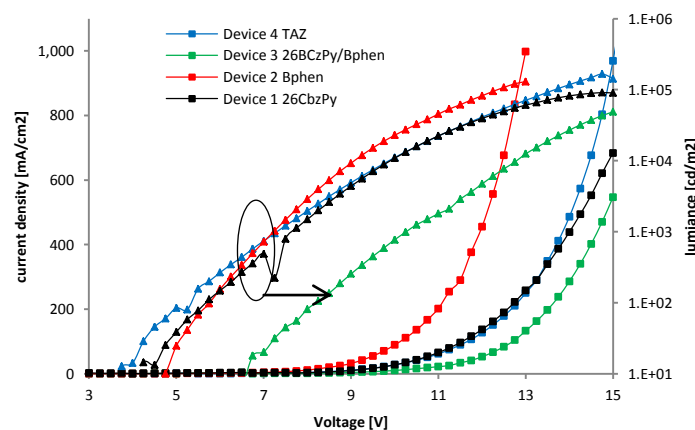


**Figure 7:** Current density-voltage-luminance (J-V-L) characteristics for blue FIrpic/o-CBP based devices 1-4.

While devices 3 with double electron transport layers of 2,6-BCzPy and BPhen (device 3) shows poorest performance regarding both turn-on voltage and luminance significant changes are observed when BPhen (device 2) is used by itself (Figure 7). The turn-on voltage is decreased from 7 V to less than 5 V and the luminance of the system is increased by almost two orders of magnitude. Compared to that, single electron transport layer devices 1 (2,6-BCbzPy) and 4 (TAZ) exhibit even higher luminance at lower voltage while having almost identical turn-on voltages of around 4 eV. This trend is more obvious by looking at luminance, -external quantum efficiency (EQE) and -power efficiency versus current density characteristics in Figure 8 a,b,c.

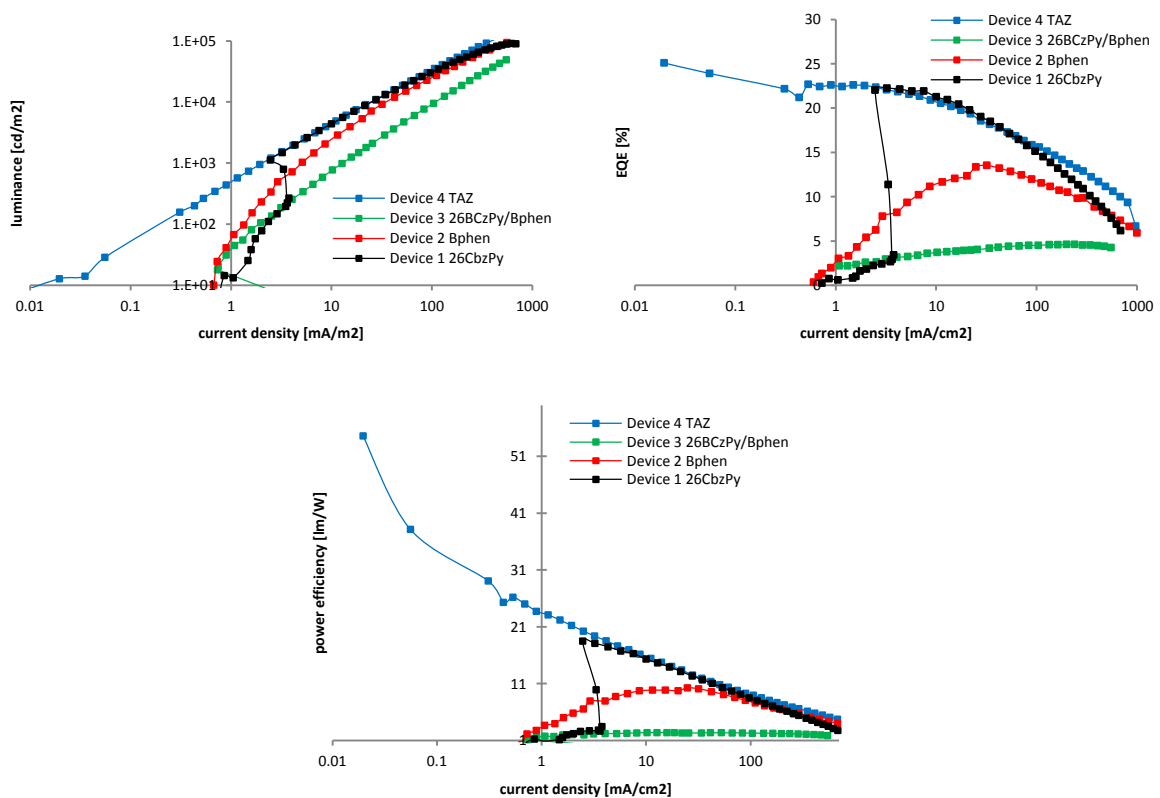


**Figure 8:** a) luminance/ b) EQE/ and c) power efficiency versus current density characteristics for blue FIrpic/o-CBP based devices 1-4; data was corrected for better signal to noise ratio

Devices 4, 1 and 2 show superior luminance characteristics over double electron transporting layer device 3 over the entire operating current regime, averaging at least one order of magnitude higher luminance (Figure 8a). Although, device 4 is the only one experiencing also good luminance performance at (important) very low (>1mA/cm<sup>2</sup>) current densities, devices 4, 1 and 2 become almost indistinguishable at higher values. However, when comparing EQE and power efficiency characteristics (Figure 8a&b) the difference in performance becomes more obvious. Again at low current device 4 shows best performance resulting in an EQE value of 22% and a

peak power efficiency of 54 lm/W, putting this system well within the range of commercial blue LEDs<sup>22,23</sup>.

The worse performance of device 1 is most likely attributed to electrical contacting problems, as the performance is comparable with that of device 4 after a sharp onset at 3 mA/cm<sup>2</sup>. Devices 2 and especially 3 show inferior performance concerning EQE and power efficiency. This is attributed to the better LUMO alignment in respect to the CsF/Al cathode as well as a higher electron transporting mobility of TAZ and 2,6-BCbzPy respectively. Less power is lost for electron injection to break the energy difference between the LUMO of the ETL and the cathode system. While device 2 (BPhen) possesses very similar energy values in respect to electron injection as device 4 (TAZ)(Figure 4), the intrinsic difference of electron transporting ability manifests in the much poorer device performance. The concept of successively lowering the electron injection barrier using two electron transporting layers (device 3) clearly fails, even though each material by itself (device 1; device 2) is performing reasonably well.

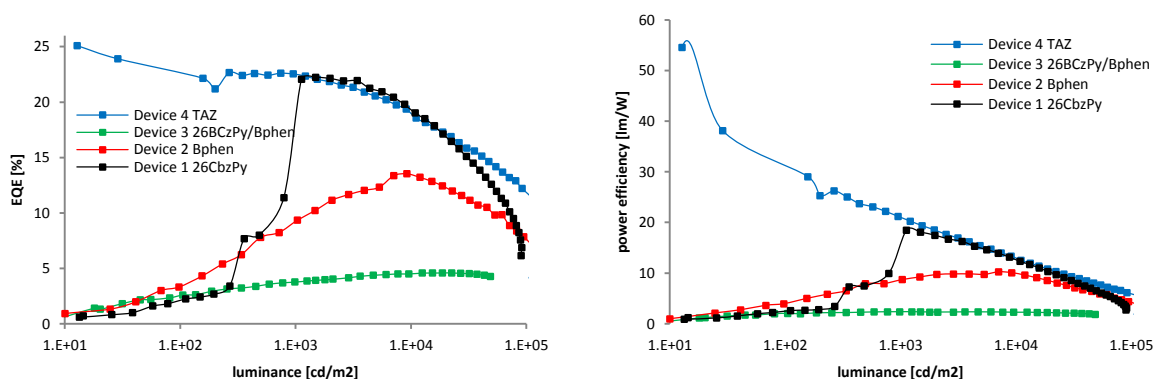


**Figure 9:** a) EQE/ and -b) power efficiency versus luminance characteristics for blue Flrpic/o-CBP based devices 1-4; data was corrected for better signal to noise ratio

In order to evaluate these devices in the context of industrial applicability and performance, EQE- and power efficiency versus luminance characteristics are displayed (Figure 9), underlining once again the supremacy of device configuration 4 followed by device 1.

Table 2 converts the data of the previously shown graphs into numeric values. The outstandingly good values of device 4 at very low current densities have to be noted with some care. High noise ratios in this regime combined with very low applied currents require precise calibration and control of the measurement device.

Nevertheless, as device 4 also exhibits exceptional performance at higher current density values, the supremacy of this configuration, based on optimized charge carrier injection and energy alignment with neighboring layers, has to be acknowledged and will be considered in further studies.

Device	Turn-on [V]	Max. luminance [cd/m <sup>2</sup> ]	Max. EQE [%] as f(J)*	Max. PE [lm/W] as f(J)*	EQE (%) at 100, 1000, 10000, 100000 cd/m <sup>2</sup>
1	4.0	90930	22.0 (2.5)	18.5 (0.02)	2, 22, 19, 7
2	4.2	130165	13.5 (31.9)	10.2 (24.9)	3, 9, 14, 8
3	6.5	48895	4.6 (238.0)	2.38 (15.8)	3, 4, 5, na
4	3.5	165620	25.1 (0.5)	54.6 (15.8)	22, 22, 19, 12

**Table 2:** characteristics for device configurations 1-4; \*J=current density [mA/cm<sup>2</sup>]

The above mentioned results suggest that o-CBP is a suitable and readily available host material for Flrpic in a PHOLED device (Figure 10). However, in order to achieve high performing devices a number of parameters as well as charge transporting materials and their interactions amongst each other have to be considered and optimized. It's noteworthy to mention that in this study the focus was to investigate o-CBP as host material for blue phosphorescent dopants (e.g, Flrpic). Higher performances could be obtained using light outcoupling techniques<sup>1,24</sup>, additional or other ETL materials or optimizing fabrication parameters (deposition rate, layer thickness etc).

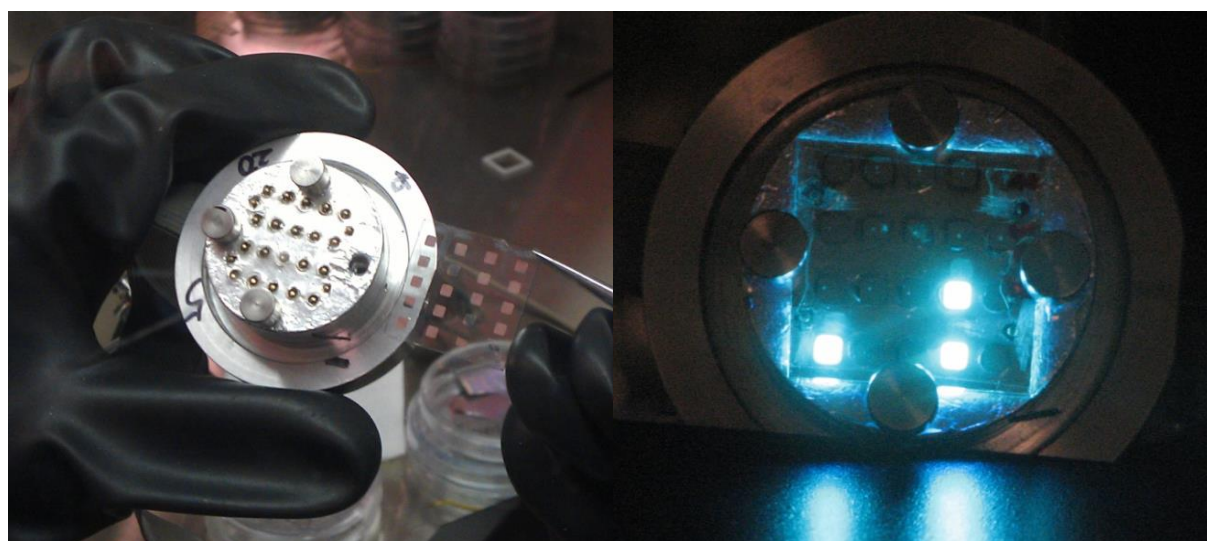


**Figure 10:** left: Device testing setup; right: three working pixels of device configuration 4

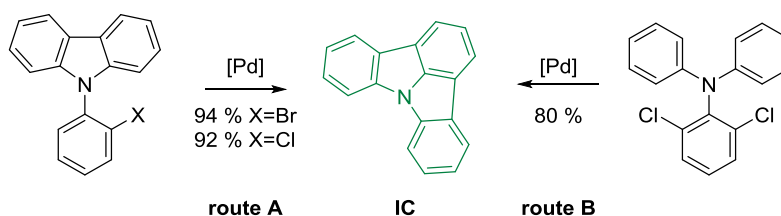


## D) Indol[3,2,1-*jk*]carbazole (IC) investigations

The advantageous properties ( $E_T$ ) of *o*-CBP and the thus resulting good device performances can be attributed to the combined concepts of ortho-linkage and planarization<sup>19</sup>.

The latter concept is taken to the extreme when introducing the novel, completely planarized substance class of indol[3,2,1-*jk*]carbazole (IC) (Scheme 2, Figure 11), which was a target compound in the diploma thesis of the scholar<sup>21</sup>.

Scheme 2 shows the newly designed and highly efficient routes towards IC by one and two fold C-H activations by applying (NHC)Pd(allyl)Cl as catalyst.



**Scheme 2:** route A: palladium catalyzed one fold C-H activation<sup>21</sup>; route B: newly developed intermolecular tandem cyclization from proper chlorine precursor

Figure 11 illustrates the complete planarity of the IC system again. The only atoms reaching out of plane are those belonging to the boronic ester group, used for following Suzuki coupling reactions.

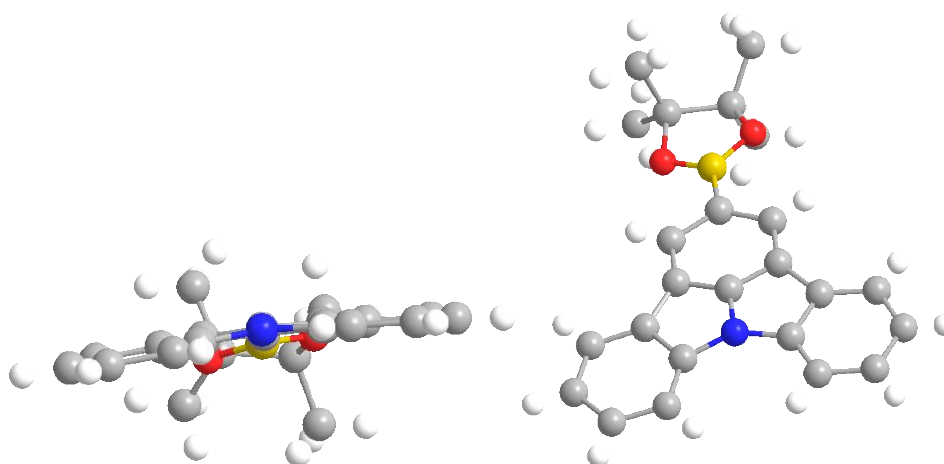


**Figure 11:** Crystal structure of 2-(4,4,5,5-tetramethyl-1,3,2-dioxaborolan-2-yl)indolo[3,2,1-*jk*]carbazole; side and front view

In cooperation with Prof. Anzenbacher the IC moiety was investigated regarding its properties as organic electronic material (e.g host material, semiconductor).

In a first step the bandgap (HOMO-LUMO energy difference) of IC was determined, via cyclic voltammetry (CV) and UV/VIS absorption spectra (Figure 12), giving a first indication of possible applications (e.g. if the bandgap is small enough the material is suitable as an organic semiconducting material).

The HOMO energy level in reference to ferrocene<sup>i</sup> was determined to be -5.77 eV, while the LUMO was calculated according to the equation  $E_{\text{LUMO}} = E_{\text{HOMO}} + E_{\text{g}}$  where  $E_{\text{g}}$  was extracted from the onset of the absorption spectrum in solution. The optical band gap from the UV/VIS spectra is 3.26 eV resulting in a LUMO level of -2.51 eV. Additionally the triplet energy ( $E_{\text{T}} = -2.86$  eV) was determined at 77 K from phosphorescent measurements along with fluorescence- (7 ns) and phosphorescence- (5.4 s) lifetimes.

HOMO [eV]	LUMO [eV]	$E_{\text{g}}$ [eV]	$E_{\text{T}}$ [eV]	$\tau_{\text{FL}}$ [ns]	$\tau_{\text{PL}}$ [s]
-5.77	-2.51	3.26	2.86	7	5.4

**Table 3:** photophysical properties of IC

Fluorescence and phosphorescence spectra were recorded using a single-photon-counting spectrofluorimeter from Edinburgh Analytical Instruments (FLSP 920) equipped with a pulsed xenon flash-lamp (mF920H, 200–900 nm, 10–100 Hz) for time-gated experiments. For phosphorescence studies at 77 K, the samples were dissolved in a 9:1 mixture of spectroscopic grade EtOH and MeOH and converted into a glass using liquid nitrogen. The samples were placed in quartz EPR tubes (Norrell) and immersed in a Dewar with liquid nitrogen. The signal acquisition of the photomultiplier tube was electronically gated to avoid saturation of the detector by fluorescence.

<sup>i</sup> A  $10^{-3}$  M solution of the sample in dry acetonitrile was prepared using ferrocene as reference and tertbutylammoniumhexafluorophosphate (TBAP, 0.1 M) as supporting electrolyte.

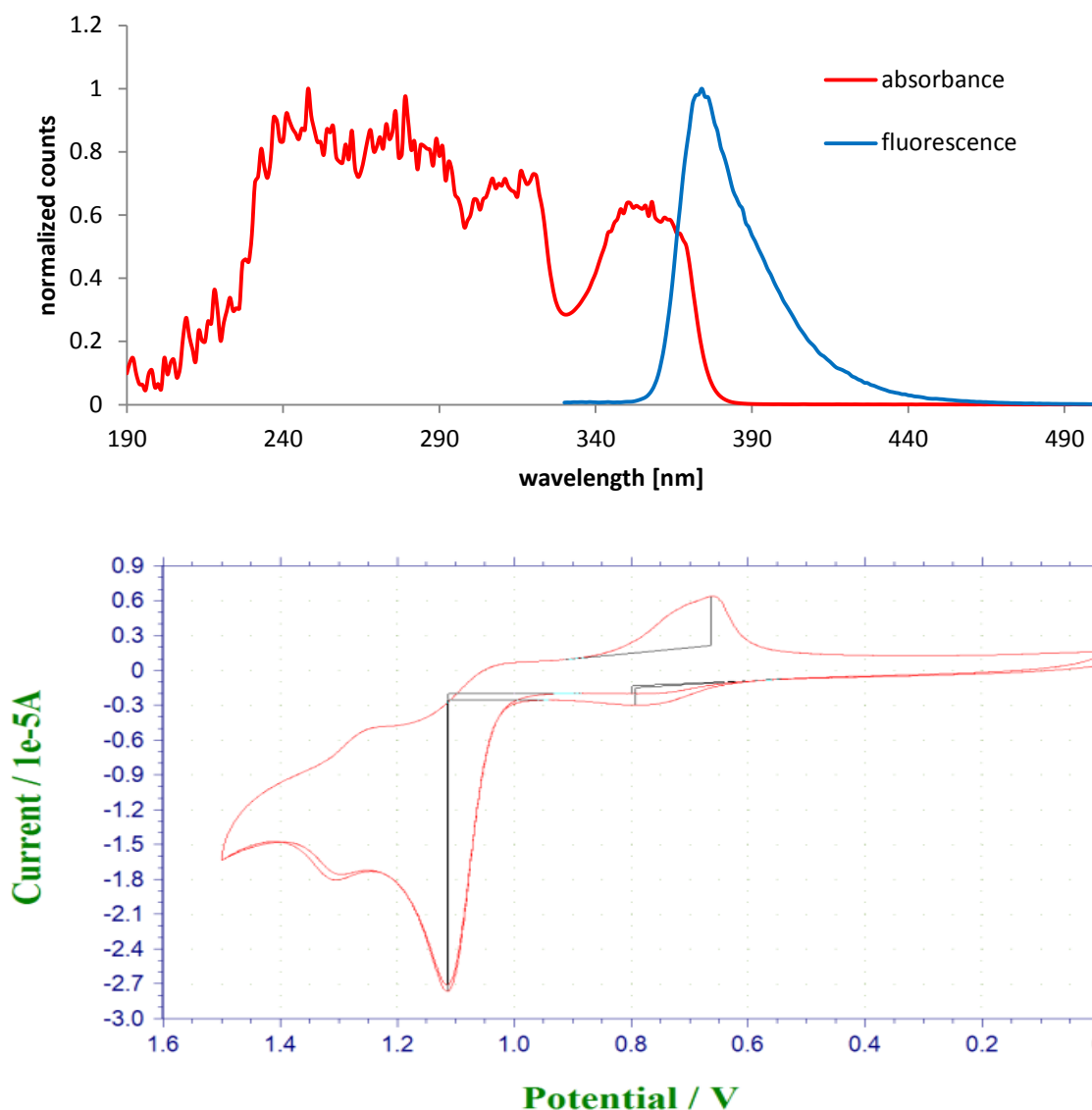


**Figure 12:** top: UV/VIS absorption and fluorescence emission spectra of IC as  $10^{-5}$  M solution in EtOH/MeOH=9:1; bottom: cyclic voltammetry measurement of IC in acetonitrile and TBAP (tetrabutylammonium hexafluorophosphate) as electrolyte

These results suggest a bandgap too large for good semiconducting purposes, however relatively high triplet energy making this compound suitable as a host material for green or even blue PHOLEDs.

The very narrow emission spectrum of IC is attributed to the very rigid nature of the molecule (Figure 12) which doesn't allow many degrees of freedom and therefore only few vibrational modes.

In a first test IC was used as host material for green emitter Ir(ppy)acac with specifications listed in Table 4.

Layer	Material	Thickness [Å]	Rate [Å/s]	Power [%]
1	ITO	3000		
2	PEDOT:PSS	300		
3	NPD	300	1.0	8.7
4	mCP	50	0.28	6.5
5	IC	315	0.36	0.6
5	Ir(ppy)acac	35	0.04	122°C
6	TPBI	300	0.3	155°C
7	BPhen	150	0.3	120°C
8	CsF	15	0.14	13.8
9	Al	1350	2.9	6

**Table 4:** Table of individual layer materials and their corresponding thicknesses, deposition rates and required power

Figure 13 illustrates the corresponding energy levels of the individual layers of the IC-PHOLED device. The HOMO-LUMO levels of IC meet the requirements as host material for Ir(ppy)acac. However, due to the low molecular weight and thus resulting relatively high volatility of IC (evaporation power 0.6%), the material didn't endure the depositions of the following layers. Therefore no working PHOLED device could be fabricated using IC.

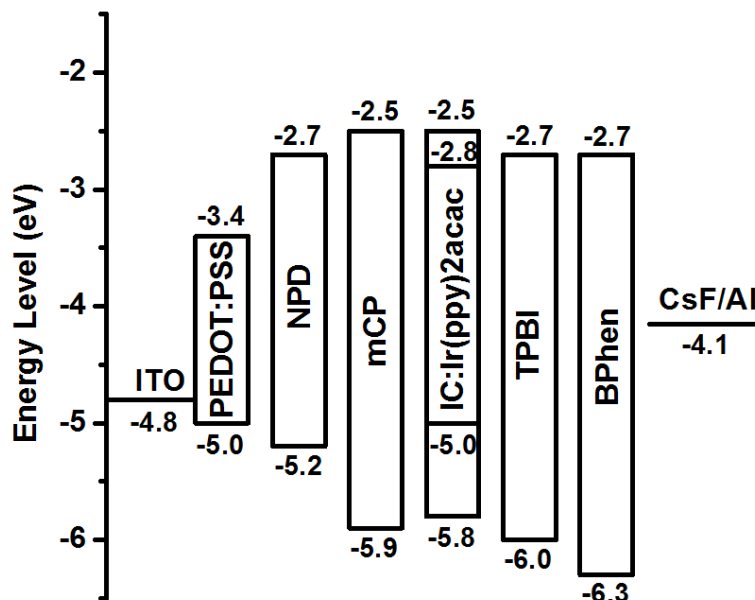


**Figure 13:** Energy levels of the multilayer PHOLED device

## Outlook

This result is unfortunate, but inspired by the fact that recently the IC moiety was recently used in a number of patents from companies like Kodak, Canon, Fujifilm and Merck<sup>25-31</sup> as an organic electroluminescence device material due to its extraordinary properties we are excited to have a reliable and highly efficient synthetic methodology at hand in order to commence further studies on this material. Figure 14 shows some of the new compounds based on IC which are on the way in order to explore the unique characteristics of the IC moiety. The intention of these materials is to maintain the high triplet energy of the IC class while increasing the molecular weight and therefore the stability.

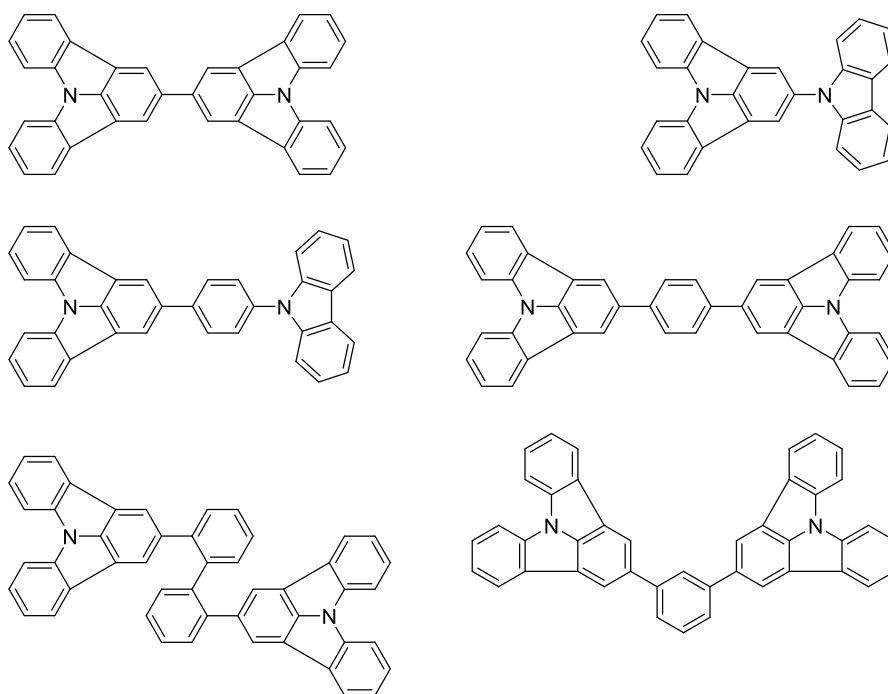


**Figure 14:** intended new compounds based on the IC moiety

## E) Conclusion

Two related projects within the field of organic electronic host materials were investigated.

Host material **o-CBP** was successfully synthesized, via a newly developed two step reaction protocol, and employed as guest matrix for blue phosphorescent emitter Flrpic in a multilayer PHOLED. Additionally, three different materials (TAZ, BPhen, 2,6-BCzPy) were tested in the context of device architecture optimization via electron transporting layer modifications. Device 4, using TAZ and o-CBP/Flrpic appears to be the best configuration achieving record values of 54 lm/W power efficiency, 22 % EQE, 3.5 eV turn-on voltage and 165620 cd/m<sup>2</sup> maximum luminance.

This can be attributed to both the high triplet energy (3.02 eV) of o-CBP, confining the triplet exciton on the Flrpic and its matched HOMO level (5.60 eV) to facilitate hole injection to the emitting layer. These results demonstrate that simple modification of the linking topology between the carbazole unit and the central biphenyl group of CBP is an effective approach to design thermally and morphologically stable host materials with high triplet energies for highly efficient blue PhOLEDs<sup>20</sup>.

In the second project recently synthesized indol[3,2,1-jk]carbazole (**IC**) was investigated as potential new host material. Electrochemical and photophysical properties of this new compound were determined using cyclic voltammetry and phosphorescence spectroscopy. Its high triplet energy (2.86 eV) and good HOMO-LUMO levels (-5.77;-2.51 eV) makes it a suitable host material for green and maybe even blue PHOLEDs. However, due to its low molecular weight and therefore high volatility the compound did not endure the fabrication process and no working PHOLED could be obtained. Nevertheless, the properties of IC are very promising and with the newly developed synthetic protocol at our disposal a number of new host materials will be available shortly.

Finally, I would like to extend my greatest appreciations to the Marshal Plan Foundation for the financial support and the unique opportunity to broaden my scientific horizon. Besides my organic synthetic capabilities I acquired a new skillset in the emerging field of organic electronics and learned so much in the process of this project. It was a very awarding and fantastic experience.

## F) Bibliography

- (1) Reineke, S.; Lindner, F.; Schwartz, G.; Seidler, N.; Walzer, K.; Lussem, B.; Leo, K. *Nature* **2009**, *459*, 234–238.
- (2) Nuyken, O.; Jungermann, S.; Wiederhorn, V.; Bacher, E.; Meerholz, K. *Monatshefte Für Chem. - Chem. Mon.* **2006**, *137*, 811–824.
- (3) Meerholz, K. *Nature* **2005**, *437*, 327–328.
- (4) Tao, Y.; Yang, C.; Qin, J. *Chem. Soc. Rev.* **2011**, *40*, 2943–2970.
- (5) Sun, Y.; Giebink, N. C.; Kanno, H.; Ma, B.; Thompson, M. E.; Forrest, S. R. *Nature* **2006**, *440*, 908–912.
- (6) Kammoun, A. *Organische Leuchtdioden aus Polymeren und niedermolekularen Verbindungen für grossflächige OLED-Anzeigen*; 1. Aufl.; Cuvillier: Göttingen, 2008.
- (7) Chou, P.-T.; Chi, Y. *Chem. – Eur. J.* **2007**, *13*, 380–395.
- (8) Chen, F.-C.; He, G.; Yang, Y. *Appl. Phys. Lett.* **2003**, *82*, 1006–1008.
- (9) Tokito, S.; Iijima, T.; Suzuri, Y.; Kita, H.; Tsuzuki, T.; Sato, F. *Appl. Phys. Lett.* **2003**, *83*, 569–571.
- (10) Kwak, J.; Lyu, Y.-Y.; Lee, H.; Choi, B.; Char, K.; Lee, C. *J. Mater. Chem.* **2012**, *22*, 6351.
- (11) Baldo, M. A.; Adachi, C.; Forrest, S. R. *Phys. Rev. B* **2000**, *62*, 10967–10977.
- (12) Peng, Q.; Chen, P.; Li, F. *Appl. Org. Electron. Photonics* **2013**, *6*, 9–9.
- (13) Shirota, Y.; Kageyama, H. *Chem Rev* **2007**, *107*, 953–1010.
- (14) Chaskar, A.; Chen, H.-F.; Wong, K.-T. *Adv. Mater.* **2011**, *23*, 3876–3895.
- (15) Evgueni Polikarpov, A. B. P. *Mater. Matters 712-8* **2012**.
- (16) Mamada, M.; Ergun, S.; Pérez-Bolívar, C.; Anzenbacher, P. *Appl. Phys. Lett.* **2011**, *98*, 073305–073305–3.
- (17) Sajoto, T.; Djurovich, P. I.; Tamayo, A.; Yousufuddin, M.; Bau, R.; Thompson, M. E.; Holmes, R. J.; Forrest, S. R. *Inorg. Chem.* **2005**, *44*, 7992–8003.
- (18) Tao, Y.; Wang, Q.; Yang, C.; Zhong, C.; Zhang, K.; Qin, J.; Ma, D. *Adv. Funct. Mater.* **2010**, *20*, 304–311.
- (19) He, J.; Liu, H.; Dai, Y.; Ou, X.; Wang, J.; Tao, S.; Zhang, X.; Wang, P.; Ma, D. *J. Phys. Chem. C* **2009**, *113*, 6761–6767.
- (20) Gong, S.; He, X.; Chen, Y.; Jiang, Z.; Zhong, C.; Ma, D.; Qin, J.; Yang, C. *J. Mater. Chem.* **2012**, *22*, 2894–2899.
- (21) Bintinger, J. *Sterically tuned triaryl amines and oligothiophene derivatives as building blocks for novel organic electronic materials: synthesis and characterization*, Vienna University of Technology, 2011.
- (22) *Solid-State Lighting Research and Development: Manufacturing Roadmap*, U.S. Department of Energy, 2011 **2011**.
- (23) Tyan, Y.-S. *J. Photonics Energy* **2011**, *1*, 011009–011009.
- (24) Shinar, J.; Shinar, R. *J. Phys. Appl. Phys.* **2008**, *41*, 133001.
- (25) Sekiguchi, T.; Ohnishi, H.; Muratsubaki, M. AMINOINDOLO[3,2,1-jk]CARBAZOLE COMPOUND AND ORGANIC LIGHT-EMITTING DEVICE INCLUDING THE SAME. WO2013018530 (A1), February 7, 2013.
- (26) Abe, S.; Kamatani, J.; Kishino, K. Indolo[3,2,1-Jk]carbazole Compound and Organic Light-Emitting Device Containing the Same. US2012075273 (A1), March 29, 2012.
- (27) Parham, A. H.; Pflumm, C.; Brocke, C. Compounds for Electronic Devices. DE102010005697 (A1) Abstract of corresponding document: WO2011088877 (A1), July 28, 2011.

- (28) Fanghaenel, E.; Hinh, L. V.; Alsleben, I.; Ackermann, R.; Richter, A. M. New tris(hydroxynaphthylazo) bridged triphenylamine pigments for electrophotographic charge generating layer. DE19808088 (A1), August 26, 1999.
- (29) Pycene-Based Compound, Organic Electroluminescent Element and Illuminating System. JP2012236786 (A), December 6, 2012.
- (30) Organic Electroluminescent Element Material, Organic Electroluminescent Element, Display Device, and Lighting Device. JP2012234873 (A), November 29, 2012.
- (31) Organic Electroluminescent Element, Display Device, and Lighting Device. JP2012191031 (A), October 4, 2012.

## Appendix

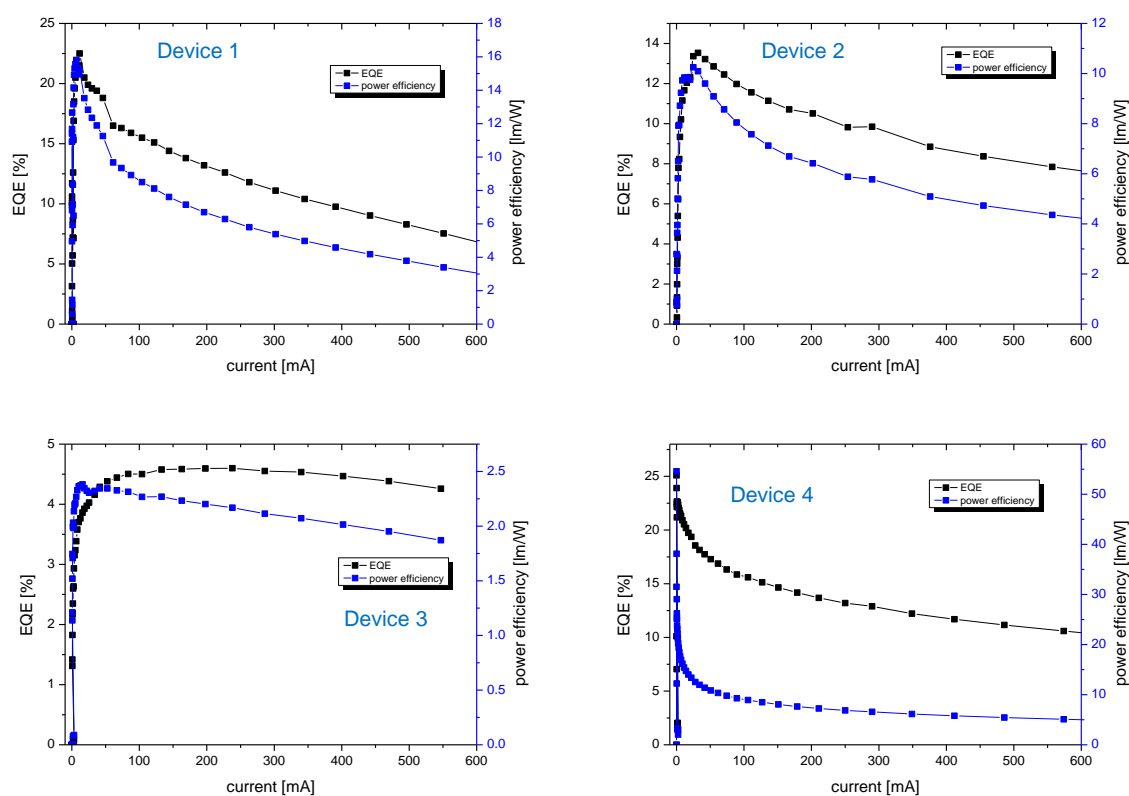


Figure 15: individual EQE-J-L characteristics of o-CBP/Flrpic devices 1-4